

## Superconducting dc transformer coupling\*

Max D. Sherrill and William A. Lindstrom†

Department of Physics and Astronomy, Clemson University, Clemson, South Carolina 29631

(Received 8 July 1974)

Measurements of the ratio of secondary voltage to primary voltage as a function of the secondary current allow a determination of the superconducting dc transformer coupling force. The force was measured for tin-film transformers. The primary film thickness and the thickness of the SiO insulating layer were varied. The maximum coupling force appears to be given approximately by  $F_{cm} \simeq (\phi_0^2/8\pi\mu_0) \times [\lambda_p \coth(d_p/\lambda_p) + \xi_p + d_0]^{-1} [\lambda_s \coth(d_s/\lambda_s) + \xi_s + d_0]^{-1}$ . Here  $d_0$ ,  $d_p$ , and  $d_s$  are the oxide thickness, primary thickness, and secondary thickness, and other symbols are standard.

### I. INTRODUCTION

Two planar, superposed, but insulated superconducting films act as a superconducting dc transformer.<sup>1-7</sup> Fluxons penetrate both films so that a current in one film induces fluxon motion in both and a flux-flow voltage appears in both. The transformer operates because of the coupling force exerted upon a fluxon in the secondary film due to a displacement of the fluxon in the primary film.

In the present experiments a quantity which is approximately equal to the maximum coupling force is measured for tin-film transformers. The measurements were made on a number of transformers in which the primary film thickness was varied from 30 nm (300 Å) to 400 nm and the separation between the films was varied from 30 to 1500 nm. The approximate value of the coupling force was obtained by sending currents in opposite directions in the two films. The secondary current density  $J_{s0}$  which is just sufficient to completely destroy the coupling leads to a force  $J_{s0}\phi_0 d_s$  which the coupling force cannot overcome. Here  $\phi_0$  is the flux quantum and  $d_s$  is the thickness of the secondary film.

Recently, Ekin, Serin, and Clem<sup>8</sup> have determined the coupling force as a function of magnetic field and temperature for a transformer made from two 74-nm granular aluminum films separated by 12 nm of silicon monoxide. They determine the force by comparing the dynamical behavior of their transformer with a theory of coupled fluxon arrays developed by Clem.<sup>9</sup> This determination was possible because their transformers were distinguished by very small pinning forces so that heating effects were negligible.

The present measurements, which were made with no applied magnetic field, differ from those of Ekin *et al.* in that the films are intrinsically type I, are sometimes thicker than the penetration depth  $\lambda$ , are sometimes separated by large distances, and have coherence lengths  $\xi$  which are larger than  $\lambda$ . Further, the pinning forces are large so that heating is not negligible except in the limit of zero

voltage.

In Sec. II we describe the preparation of the samples. In Sec. III the measurements are described and the experimental results are presented. In Sec. IV an expression for the coupling force on an isolated fluxon<sup>10</sup> which is valid in the thin-film limit ( $d \ll \lambda$ ,  $\xi \ll \lambda^2/d$ ) with the films close together is empirically modified so that it is applicable also to thick widely separated films with large fluxon cores. The results are compared with this expression and with the results of Ekin *et al.* to which the thin-film approximation is applicable.

### II. SAMPLE PREPARATION

The transformers used in these experiments consisted of two tin films insulated from each other by a film of silicon monoxide. The films were produced by vapor deposition of 99.999%-pure tin and vacuum degassed SiO onto glass microscope slides which were nominally at room temperature. The pressure in the evaporator was approximately  $4 \times 10^{-6}$  Torr during the tin deposition and approximately  $1.5 \times 10^{-5}$  Torr during the SiO deposition. All films were deposited at a rate of approximation 100 nm per minute.

The sample configuration used is shown in Fig. 1. First, indium patches were soldered to the substrate to allow for a four-probe measurement of the  $I$ - $V$  characteristics of each film. Next, a tin film was deposited on the slide which was masked so that the tin covered all but about 1 cm at each end of the slide. The SiO was deposited so that it covered the entire film. A long narrow secondary tin film was deposited in the center of the slide. After each tin evaporation, Pb films were deposited on the tin in the region of contact with the indium patches. This ensured superconducting contacts to the tin films. The first tin film was then scribed as shown in Fig. 1 to produce three primary films which shared the single long secondary film. The sample dimensions are given in Table I.

As shown in Table I the samples were produced in two groups. In the first group the insulator

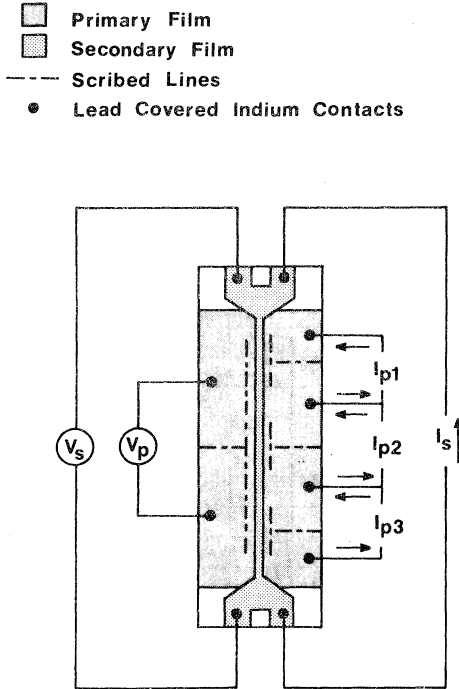


FIG. 1. Schematic drawing of a sample.

thickness was varied from 25 to 1500 nm while the primary and secondary thicknesses were kept fixed at 400 and 200 nm, respectively. In preparing these samples a movable mask was used during the SiO evaporation so that the three transformers on a slide each had a different insulator thickness. In the second group of samples the SiO thickness was fixed at 30 nm and the secondary thickness at 200 nm while the primary film thickness was varied from 48 to 400 nm. Also three transformers with 20-nm primaries were produced with the substrate at 77 K during the primary film deposition. These primary films were produced at a rate of 15 nm per minute.

### III. MEASUREMENTS

The objective of the measurements reported here was to determine the maximum coupling force in superconducting transformers and how it depends upon some of the transformer parameters. This force depends upon the thickness of the primary film  $d_p$ , the secondary film  $d_s$ , and the oxide film  $d_o$ , and the temperature-dependent penetration depths and coherence lengths  $\lambda_p$ ,  $\lambda_s$ ,  $\xi_p$ ,  $\xi_s$ . The coupling force decreases with applied magnetic field<sup>4,5,8</sup> so that its maximum value occurs at zero field. All of the measurements presented here were made with *no* applied magnetic field. There was of course the self-field of the currents in the films. We estimate that in extreme cases the max-

imum self-field was approximately  $3 \times 10^{-4}$  T (3 G) perpendicular to the primary film at its edges.

The samples were placed in a glass cryostat and attached to external circuitry which could supply currents to both primary and secondary films and display on an *x-y* plotter the following characteristics: the primary voltage  $V_p$  or secondary voltage  $V_s$  as a function of the germanium-resistance-thermometer voltage,  $V_p$  or  $V_s$  as a function of primary current  $I_p$ ,  $V_s$  as a function of secondary current  $I_s$ , and  $V_s$  as a function of  $V_p$  with  $I_s$  as a parameter. The film resistances were measured at room temperature, 77, and 4.2 K. The transition temperatures of all films were determined and then the transformer characteristics were measured at several temperatures.

The transition temperatures of the primary films ranged from about 3.85 to about 3.95 K. The transition temperatures of the secondary films ranged from about 3.75 to about 3.83 K. The primary films always had higher transition temperatures than the secondary films. The resistivities of the films ranged from  $0.45 \times 10^{-8}$  to  $2.24 \times 10^{-8}$   $\Omega$  m at 4.2 K.

The range of temperatures in which useful data could be obtained was limited by heating effects.<sup>1,5,8</sup> As the temperature was lowered the primary depinning current increased and heating determined the maximum primary current for transformer function. When the temperature was sufficiently low the primary would make an abrupt transition to the normal state when the depinning current was reached. This effect was less severe in some samples but we obtained no useful data below relative primary temperatures  $T/T_c$  of 0.94. The measured primary depinning currents for all samples and temperatures ranged from 0.01 to 0.5 A.

In transformers made from type-I films with such large depinning currents the  $I_p$ - $V_p$  and  $I_p$ - $V_s$  characteristics are strongly influenced by heating

TABLE I. Sample dimensions and characteristics.

	Length (mm)	Width (mm)	Material
Substrate	75	25	glass
Primary	10.5	1.40	tin
Secondary	52.3	0.91	tin
Insulator	...	...	SiO
Group-I samples:			
Thickness <sup>a</sup> (nm)	Primary	Secondary	Insulator
	400	200	250-1500
Group-II samples:			
Thickness <sup>a</sup> (nm)	Primary	Secondary	Insulator
	30-400	200	30

<sup>a</sup>Measured with a Sloan deposit thickness monitor (DTM-3).

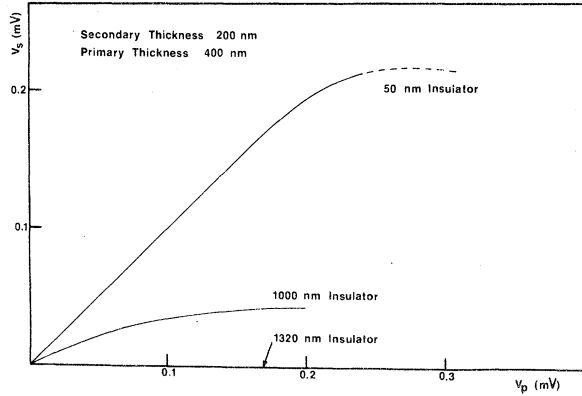


FIG. 2. Secondary voltage as a function of primary voltage with insulator thickness as the parameter.

effects. Such characteristics have been presented before<sup>1-6</sup> and further they cannot easily be interpreted in detail.<sup>8</sup> We will present here plots of  $V_s$  as a function of  $V_p$  with oxide thickness, primary thickness, and secondary current as parameters. When  $V_p$  and  $V_s$  are zero then the heating is also zero so we will be concerned primarily with the initial slopes  $(V_s/V_p)_0 = \lim_{V_p \rightarrow 0} (V_s/V_p)$  of these plots.

In Fig. 2 the open-circuit secondary voltage  $V_s$  is shown as a function of  $V_p$  for three transformers with different insulator thicknesses. Figure 3 shows a similar plot for three transformers with different primary thicknesses. The characteristics vary with the temperature so we have shown them for each transformer at the temperature for which  $(V_s/V_p)_0$  was largest. One noteworthy feature of these results is that for weakly coupled transformers  $(V_s/V_p)_0$  may have values between zero and unity. Since the primary fluxon velocity approaches zero as  $V_p$  approaches zero, this must be due to the nature of the secondary pinning forces rather than the viscous drag force. This behavior of weakly coupled transformers has been discussed before.<sup>7,11</sup>

The transformer coupling may be reduced by a secondary current which is in the opposite direction to the primary current. This is shown in Fig. 4 for a transformer with a 503-nm insulating film and a 400-nm primary film. In Fig. 5 similar results are shown for a transformer with a 30-nm insulating film and a 77-nm primary. The results shown in Figs. 2-5 show that transformers with thin primary films and thin oxides behave much like those with thick primaries and thick oxides. The coupling is reduced in either case.

To obtain a measure of the coupling force we wish to determine the secondary current which reduces  $(V_s/V_p)_0$  to zero. The force applied to a secondary fluxon by the secondary current is  $J_s \phi_0 d_s$ . In Fig. 6 we show  $(V_s/V_p)_0$  as a function of secondary cur-

rent for two transformers, both of which have rather thin primary films. This kind of plot was constructed for 13 transformers in which it was possible to reduce the coupling to zero.  $(V_s/V_p)_0$  always decreased approximately linearly with secondary current.  $I_{s0}$  is the secondary current which reduces the coupling to zero and  $J_{s0}$  the corresponding current density. Figure 5 also shows that when the coupling is imperfect it may be improved with a secondary current which is in the same direction as the primary current. In Sec. IV we will attempt to relate  $J_{s0} \phi_0 d_s$  to the maximum coupling force  $F_{cm}$ .

#### IV. COUPLING FORCE

The measured values of the primary and secondary depinning currents indicated that the primary pinning forces were always larger than the secondary pinning forces or the coupling forces. If the secondary pinning forces were all identical and therefore characterized by a single pinning force per fluxon  $F_{ps}$ , one could then write

$$F_{ps} + F_{cm} = J_{ps} \phi_0 d_s, \quad F_{cm} < F_{pp}. \quad (1)$$

Here  $J_{ps}$  is the measured secondary depinning current density with no current in the primary. Further one can measure  $J_{s0}$ , the secondary current density which destroys the coupling. This gives another equation:

$$F_{ps} + J_{s0} \phi_0 d_s = F_{cm}, \quad F_{cm} < F_{pp}. \quad (2)$$

Equations (1) and (2) would then give  $F_{cm} = \phi_0 d_s (J_{s0} + J_{ps})/2$  and  $F_{ps} = \phi_0 d_s (J_{ps} - J_{s0})/2$ .

If the pinning were this simple one could therefore determine  $F_{cm}$  and  $F_{ps}$  by making two simple measurements. But this implies that the ratio  $V_s/V_p$  would always approach 1 or zero as  $V_p$  approached zero. Further,  $(V_s/V_p)_0$  would drop abruptly from unity to zero when the secondary current reached

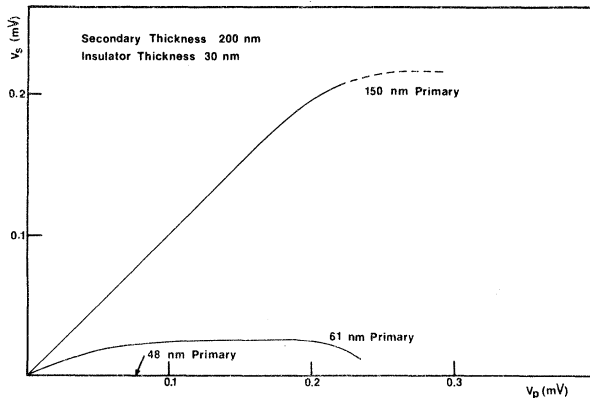


FIG. 3. Secondary voltage as a function of primary voltage with primary thickness as the parameter.

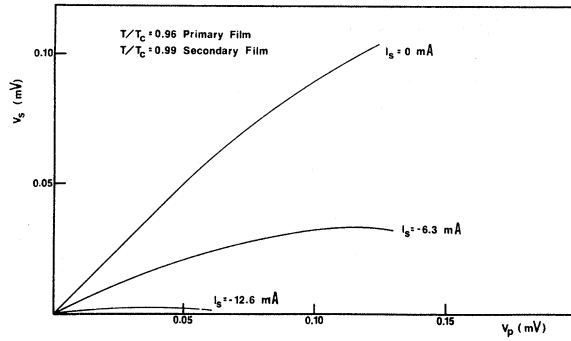


FIG. 4. Secondary voltage as a function of primary voltage with secondary current as the parameter for a sample with a 400-nm primary, 200-nm secondary, and a 503-nm insulating film.

$I_{s0}$ . Neither of these statements are true for our transformers.

These considerations lead us to the conclusion that in Eq. (1)  $F_{ps}$  should be replaced by some average pinning force while in Eq. (2) it should be replaced by a minimum pinning force since *all* of the fluxons are stationary in the secondary when  $V_s$  is zero. We, therefore, rewrite Eq. (2) as

$$F_{cm} = J_s \phi_0 d_s + F_{psm}. \quad (3)$$

The qualitative behavior of the transformers has convinced us that we cannot directly measure  $F_{cm}$  since we do not know  $F_{psm}$ . We will therefore argue that  $J_s \phi_0 d_s$  is a fair measure of  $F_{cm}$  when  $F_{psm}$  is small, and a lower limit on  $F_{cm}$  in any case.

Having measured the quantity  $J_s \phi_0 d_s$  which should be a good lower limit on the maximum coupling force, we need a model for the coupling force with which it can be compared. The coupling force for an isolated fluxon has been calculated in the thin-film approximation.<sup>10</sup> This calculation applies only

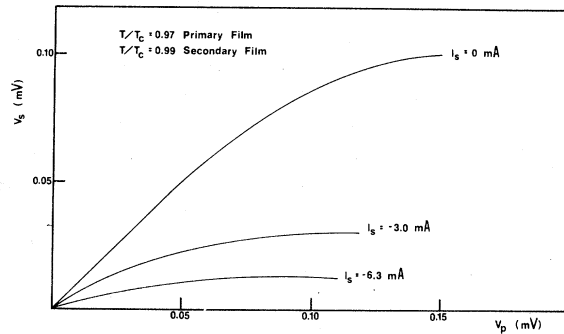


FIG. 5. Secondary voltage as a function of primary voltage with secondary current as the parameter for a transformer with a 77-nm primary, 200-nm secondary, and 30-nm insulating film.

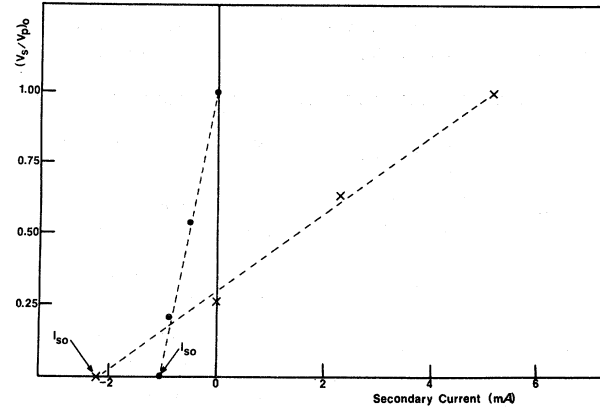


FIG. 6. Coupling parameter  $(V_s/V_p)_0$  as a function of secondary current for two transformers with 200-nm secondaries and 30-nm insulation. Dark circle: 77-nm primary. Crosses: 51-nm primary.

in the limits  $d_p, d_s, d_o, \xi \ll \lambda$ , so it is not directly applicable to the present measurements. The results is  $F_c = (\phi_0/\mu_0)(\lambda_p^2/d_p + \lambda_s^2/d_s)A(R)$ . Here  $A(R)$  is the vector potential of the fluxon and  $R$  is the distance between primary and secondary fluxon cores.  $A(R)$  has been calculated by Pearl<sup>12</sup> in the thin-film limit. In his calculation  $A(R)$  has its maximum value of  $(\phi_0/4\pi)(d_p/\lambda_p^2 + d_s/\lambda_s^2)$  at the origin. This would give  $F_{cm} = (\phi_0/4\pi\mu_0)d_p d_s / \lambda_p^2 \lambda_s^2$ . However, this form for the vector potential is physically unrealistic because it describes a fluxon in which the magnetic field is infinite at the origin. A more realistic estimate of  $F_{cm}$  is probably<sup>10</sup>

$$F_{cm} \approx \frac{\phi_0}{8\pi\mu_0} \frac{d_p d_s}{\lambda_p^2 \lambda_s^2}. \quad (4)$$

In Eq. (4), the factors  $\lambda_p^2/d_p$  and  $\lambda_s^2/d_s$  are the effective penetration depths<sup>12</sup> in the primary and secondary. The quantity  $\lambda^2/d$  is also proportional to the fluxon radius in a thin film.<sup>12</sup> Our intention is to modify these factors to make Eq. (4) more or less applicable to transformers in which  $d_p, d_s$ , and  $\xi$  are comparable to or larger than  $\lambda$  and in which the distance  $d_o$  between films may be large. The arguments we use are not rigorous and the relationship which we develop should be regarded as an approximate empirical expression for the maximum coupling force which is justified by the experimental results.

First of all the effective penetration depth in a film is  $\lambda \coth(d/\lambda)$ , which approaches  $\lambda^2/d$  when  $d$  is small. The second consideration is that in our samples the coherence length or core radius  $\xi$  is not small. We expect therefore that the effective fluxon radius might be approximately  $\lambda \coth(d/\lambda) + \xi$ , which might replace  $\lambda^2/d$  in Eq. (4) when  $d_o$  is small. The third change in Eq. (4) is necessary

TABLE II. Formulas [from Gor'kov (Ref. 13) and Goodman (Ref. 14)] and parameters used in calculations

$F_{cm}$	
$\lambda(T) = \frac{\lambda_{0L}}{[2(1-T/T_c)\chi(\rho)]^{1/2}}$	London penetration depth, $\lambda_{0L} = 3.61 \times 10^{-8}$ m
$\xi(T) = \frac{0.738\chi^{1/2}(\rho)\xi_0}{(1-T/T_c)^{1/2}}$	BCS coherence length, $\xi_0 = 2.3 \times 10^{-7}$ m
$\chi(\rho) \approx (1 + 0.752\xi_0/l)^{-1}$	Fermi velocity, $V_F = 6.5 \times 10^5$ m/sec
$\approx (1 + 0.752\xi_0\rho_r/\mu_0\lambda_{0L}^2V_F)^{-1}$	Resistivity at 4.2 K, $\rho_r$ (measured)
$\xi(T) = 9.02\chi(\rho)\lambda(T)$	Transition temp, $T_c$ (measured)

to allow for the decrease in  $F_{cm}$  with oxide thickness. This might be accounted for in an approximate way by taking the fluxon radius to be  $\lambda \coth(d/\lambda) + \xi + d_o$ . With these modifications Eq. (4) becomes

$$F_{cm} \approx \frac{\phi_0^2}{8\pi\mu_0} \left[ \left( \lambda_p \coth \frac{d_p}{\lambda_p} + \xi_p + d_o \right) \left( \lambda_s \coth \frac{d_s}{\lambda_s} + \xi_s + d_o \right) \right]^{-1}. \quad (5)$$

The formulas and constants used in calculating  $F_{cm}$  from Eq. (5) are shown in Table II.

In Fig. 7 the measured values of  $J_{s0}\phi_0d_s$  are shown as a function of  $F_{cm}$  calculated from Eq. (5) for transformers with thin oxide layers (30 nm) and 200-nm secondary films. The solid line represents  $F_{cm}$  according to Eq. (5). Note that the experimental points do not intercept the  $F_{cm}$  axis at zero, but this is the expected result according to Eq. (3). As the temperature is decreased the calculated values of  $F_{cm}$  increase so that several points are shown for some transformers.

The coupling force determined by Ekin, Serin,

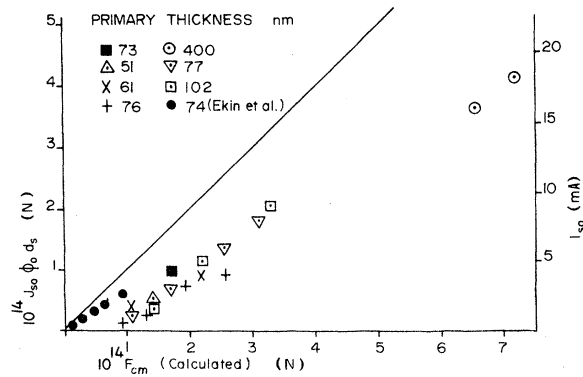


FIG. 7. Measured force which destroys the coupling as a function of  $F_{cm}$  as calculated from Eq. (5) for transformers with thin insulating films. The primary thicknesses are designated.

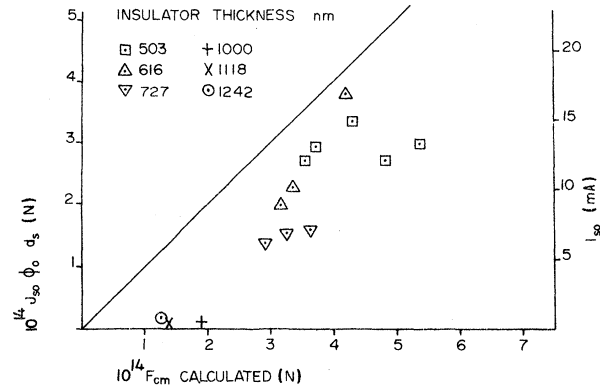


FIG. 8. Measured force which destroys the coupling as a function of  $F_{cm}$  for transformers with 400-nm primaries. The thicknesses of the insulating films are shown.

and Clem<sup>8</sup> for their transformer made from two granular aluminum films is also shown in Fig. 7. They do not report the results for zero magnetic field so we have shown their determination of  $F_{cm}$  at five different temperatures for the lowest reported magnetic field of  $2.4 \times 10^{-4}$  T (2.4 G). Their  $F_{cm}$  was determined from a best fit of their dynamical model to their data and shows the expected zero intercept.

Figure 8 shows the results for transformers with 400-nm primaries, 200-nm secondaries, and insulator thicknesses that vary from 503 to 1242 nm. Again several points are shown for some transformers. Note that the data for the two types of transformers could be presented on the same graph. However, for the results shown in Fig. 7 the effect of the oxide thickness  $d_o$  is negligible since it is small, whereas it is significant for the results shown in Fig. 8 where it is large.

Apart from the scatter in the data the results in both cases appear to agree with the loose arguments upon which Eq. (5) is based. Some of the scatter can be understood by noting the behavior of a single transformer as the calculated values of  $F_{cm}$  increase due to decreasing the temperature. In several cases  $J_{s0}\phi_0d_s$  fails to increase linearly with  $F_{cm}$  and in one case in Fig. 8 actually decreases slightly at the lower temperatures. This is probably caused by the increase in secondary pinning forces as the temperature is lowered. That is,  $F_{psm}$  becomes larger with decreasing temperature, so that it is really at higher temperatures that  $J_{s0}\phi_0d_s$  is more nearly equal to the maximum coupling force. A principal source of error and scatter in the calculation of  $F_{cm}$  is the strong dependence of  $\xi$  and  $\lambda$  and therefore  $F_{cm}$  upon temperature at high temperatures. The relative temperatures were rarely lower than 0.964 for the primaries and 0.985 for the secondaries. The transition regions were usu-

ally about 0.02 K broad.

In Fig. 7 it is clear that, apart from the intercepts, the data of Ekin *et al.* appear similar to the results reported here. For their transformers  $d_p$  and  $d_s$  were much less than  $\lambda$ , and  $\xi$  was much less than  $\lambda \coth(d/\lambda)$ , which was nearly equal to  $\lambda^2/d$ . Consequently the modifications made upon Eq. (4) to obtain Eq. (5) make little difference for their sample. For our transformers  $\xi$  was greater than  $\lambda$  and usually greater than  $\lambda \coth(d/\lambda)$ . For the data shown in Fig. 7, Eq. (4) gives values of  $F_{cm}$  which are an order of magnitude larger than  $J_{s0}\phi_0 d_s$

and leads to much more scatter. The justification for Eq. (5) is that it provides an approximate semi-empirical expression for  $F_{cm}$  which appears to apply for a wide range of coupling, and for large variations in film thickness, penetration depth, coherence length, and oxide thickness. Several other expressions for  $F_{cm}$  were compared with the measurements but none worked as well as Eq. (5). Equation (5) is, however, an expression for the maximum or optimum coupling force and will not apply when there is a large perpendicular magnetic field;  $B > (\phi_0/\pi)[\lambda \coth(d/\lambda) + \xi + d_o]^{-2}$ .

\*Research supported in part by the National Science Foundation.

†Present address: Physics Department, The College of Charleston, Charleston, S. C. 29401.

<sup>1</sup>I. Giaever, Phys. Rev. Lett. 15, 825 (1965).

<sup>2</sup>I. Giaever, Phys. Rev. Lett. 16, 460 (1966).

<sup>3</sup>P. R. Solomon, Phys. Rev. Lett. 16, 50 (1966).

<sup>4</sup>R. Deltour and M. Tinkham, Phys. Rev. 174, 478 (1968).

<sup>5</sup>P. E. Cladis, Phys. Rev. Lett. 21, 1238 (1968).

<sup>6</sup>P. E. Cladis, R. D. Parks, and J. M. Daniels, Phys. Rev. Lett. 21, 1521 (1968).

<sup>7</sup>M. D. Sherrill, Phys. Lett. A 24, 312 (1967).

<sup>8</sup>J. W. Ekin, B. Serin, and John R. Clem, Phys. Rev.

B 9, 912 (1974).

<sup>9</sup>John R. Clem, Phys. Rev. B 9, 898 (1974).

<sup>10</sup>Max D. Sherrill, Phys. Rev. B 7, 1908 (1973).

<sup>11</sup>W. A. Lindstrom and M. D. Sherrill, Phys. Lett. A 46, 77 (1973).

<sup>12</sup>J. Pearl, Appl. Phys. Lett. 16, 50 (1966); J. Pearl, *Proceedings of the Ninth International Conference on Low Temperature Physics* (Plenum, New York, 1965), Pt. A, p. 566.

<sup>13</sup>L. P. Gor'kov, Zh. Eksp. Teor. Fiz. 37, 1407 (1959) [Sov. Phys.-JETP 10, 998 (1960)].

<sup>14</sup>B. B. Goodman, Rep. Prog. Phys. 29, 445 (1966).